

Semi-continuous anaerobic digestion of mixed wastewater sludge with biochar addition

*Original*

Semi-continuous anaerobic digestion of mixed wastewater sludge with biochar addition / Chiappero, M.; Berruti, F.; Masek, O.; Fiore, S.. - In: BIORESOURCE TECHNOLOGY. - ISSN 0960-8524. - ELETTRONICO. - 340:(2021), p. 125664. [10.1016/j.biortech.2021.125664]

*Availability:*

This version is available at: 11583/2926034 since: 2021-09-21T14:59:28Z

*Publisher:*

Elsevier Ltd

*Published*

DOI:10.1016/j.biortech.2021.125664

*Terms of use:*

This article is made available under terms and conditions as specified in the corresponding bibliographic description in the repository

*Publisher copyright*

(Article begins on next page)

1 **Semi-continuous anaerobic digestion of mixed wastewater sludge with biochar**  
2 **addition**

3 Marco Chiappero<sup>a</sup>, Franco Berruti<sup>b</sup>, Ondřej Mašek<sup>c</sup>, Silvia Fiore<sup>a</sup> \*

4

5 a DIATI (Department of Engineering for Environment, Land and Infrastructures),  
6 Politecnico di Torino, Corso Duca degli Abruzzi 24, 10129, Torino, Italy

7 b Institute for Chemicals and Fuels from Alternative Resources (ICFAR), Department  
8 of Chemical and Biochemical Engineering, Faculty of Engineering, Western University,  
9 London, Ontario, N6A 5B9, Canada

10 c UK Biochar Research Centre (UKBRC), School of GeoSciences, University of  
11 Edinburgh, King's Buildings, Edinburgh EH9 3JN, United Kingdom

12

13 \*corresponding author: Prof. Silvia Fiore, DIATI, Politecnico di Torino, Corso Duca  
14 degli Abruzzi, 24; 10129, Torino, Italy; E-mail: [silvia.fiore@polito.it](mailto:silvia.fiore@polito.it); Phone: +39 011  
15 090 7613

16

17 **Abstract**

18 This work analysed the effects of biochar (BC) addition to the anaerobic digestion (AD)  
19 of wastewater mixed sludge (MS) in semi-continuous mode. A 3 L digester was  
20 operated at 37 °C for 100 days, feeding MS collected every three weeks in the same  
21 wastewater treatment plant, and 10 g L<sup>-1</sup> of BC. The average performance of MS  
22 digestion (biogas 188 NmL d<sup>-1</sup>, 68% methane) improved in presence of BC (biogas 244  
23 NmL d<sup>-1</sup>, 69% methane). According to the results of the multiple linear regression  
24 analysis performed on the experimental data, the 79% variation of the soluble COD in

25 the MS was the driving factor for the 38% increase of biogas and methane yields. In  
26 conclusion, in the considered experimental conditions, the variability of the substrate's  
27 composition was the key factor driving the performances of the AD of MS,  
28 independently of the addition of BC.

29

### 30 **Keywords**

31 biochar; biogas; linear regression; sludge; wastewater

32

### 33 **1. Introduction**

34 Wastewater treatment plants (WWTP) in Europe produce currently over 10 Mt/year of  
35 wastewater sludge (expressed as dry substance) (Eurostat, 2021). Sludge management is  
36 a critical issue for WWTPs, implying significant impacts on their operating costs  
37 (Appels et al., 2010) and environmental footprint (Gherghel et al., 2019). In the past  
38 decade, many WWTP operators have implemented AD as part of the sludge  
39 management processes to recover energy. The optimization of biogas production from  
40 wastewater sludge could heavily improve the energy balance of a WWTP (Gu et al.,  
41 2017; Jenicek et al., 2013). Even if anaerobic digestion (AD) is commonly applied in  
42 full-scale WWTPs, it still has critical issues that need to be addressed to improve its  
43 performance. Particularly in the case of waste activated sludge, the complex floc  
44 structure and the recalcitrant cell walls limit the hydrolysis and the overall  
45 implementation of AD (Zhen et al., 2017), resulting in scarce methane yields and high  
46 retention times. Further, the presence of inhibitory substances in the sludge may limit  
47 methane production (Alenzi et al., 2021; Mohammad Mirsoleimani Azizi et al., 2021).  
48 To improve the AD of wastewater sludge, different options have been widely

49 investigated, including physicochemical pre-treatments (Khanh Nguyen et al., 2021;  
50 Zhen et al., 2017), and co-digestion with other substrates (Chow et al., 2020; Elalami et  
51 al., 2019). At the same time the financial and environmental impacts of the proposed  
52 solutions (i.e., use of chemicals and energy demand) should be contained. A recent  
53 perspective in this framework considered the use of additives, mostly carbon-based  
54 materials (e.g. biochar, activated carbon, graphene, carbon fibres) (Lu et al., 2020), with  
55 the aim of improving methane production, AD stability, and digestate quality (Abbas et  
56 al., 2021). Among carbon-based additives, biochar (BC) has been receiving increasing  
57 attention due to its low cost and environmental sustainability, and the ability to increase  
58 methane yield (Chiappero et al., 2020). BC is the solid residue of the thermo-chemical  
59 pyrolytic treatment of biomass with limited or no oxygen, and it may derive from many  
60 waste biomasses (Li et al., 2019). BC has become highly attractive for many  
61 applications (Zhang et al., 2019), due to the wide variety of distinctive properties,  
62 including large surface area and porous structure, rich surface functionalities, high ion  
63 exchange capacity and adsorption ability. Specifically considering BC as additive in the  
64 AD of wastewater sludge, increased methane yields and production rates were observed  
65 (Chiappero et al., 2021). The large surface area and porous structure of BC provides a  
66 suitable habitat for microbial attachment and colonization during AD (Yin et al., 2019;  
67 Zhang et al., 2019). BC was shown to stimulate all phases of AD, from hydrolysis and  
68 acidogenesis (Wei et al., 2020; S. Xu et al., 2020; Yin et al., 2019), to acetogenesis and  
69 methanogenesis (Lü et al., 2020; Shen et al., 2021). It has been suggested that BC  
70 stimulates the syntrophic metabolisms between fermentative bacteria and methanogens  
71 (Lü et al., 2020; Shen et al., 2021) by facilitating interspecies electron transfer on its  
72 surface functional groups (Wang et al., 2020; Wang et al., 2018). Further, when

73 supplemented to the AD of wastewater sludge, BC increases the alkalinity of the  
74 system, thanks to the content of alkali and alkaline earth metals (Shen et al., 2016; Zhou  
75 et al., 2020), and mitigates ammonia inhibition (Shen et al., 2017; Zhang et al., 2019).  
76 Conversely, inhibitory effects on methane production from wastewater sludge were  
77 observed in case of excessive loads of BC by several authors (Wei et al., 2020; Wu et  
78 al., 2019; Zhang et al., 2019; Zhang and Wang, 2020). Despite the variable effects on  
79 AD due to the differences in the features of the BC, the above cited studies proved the  
80 enhancement of methane production during batch AD experiments, suggesting different  
81 potential mechanisms. Taking into account the experimental conditions involving  
82 continuously-fed digesters, the only available studies reporting positive effects of BC on  
83 methane production concerned primary sludge in thermophilic conditions (Wei et al.,  
84 2020) and temperature-phased semi-continuous AD of mixed sludge (Shen et al., 2017).  
85 To our knowledge, the effects of BC supplementation on the AD of wastewater sludge  
86 under “realistic” AD conditions (e.g., mixing primary and secondary sludge and  
87 accounting the variability of the characteristics of the sludge sampled in a certain  
88 WWTP), have not been explored yet. Full-scale WWTPs mostly feed AD with mixed  
89 sludge (primary and waste activated sludge), in continuous mode. The intrinsic high  
90 variability of the physicochemical features of the sludge in the same facility (Arhoun et  
91 al., 2019; Panepinto et al., 2016), which influences the performance of the AD, is well-  
92 known and should be considered as a key factor. The present study aims to investigate  
93 the effects of BC addition on the AD of wastewater sludge under operating conditions  
94 simulating common full-scale installations, e.g., mesophilic AD of mixed sludge  
95 sampled multiple times in the same WWTP during a period of over three months. A 3 L  
96 reactor was operated at 37 °C in semi-continuous mode over 100 days, feeding mixed

97 sludge sampled from the same WWTP every three weeks. The specific objectives of the  
98 study were: 1. investigating the effect of BC addition on raw mixed sludge (no pre-  
99 treatments), also accounting for the variability of the substrate, on biogas yield and  
100 composition; 2. exploring the relationship among BC addition, sludge biodegradability  
101 and AD performance through a linear regression approach.

102

## 103 **2. Material and Methods**

### 104 *2.1. Substrate, inoculum, and biochar*

105 Mixed sludge (MS) was sampled from a WWTP in northern Piedmont, Italy every three  
106 weeks (4 samplings in total). The MS was collected at the outflow of the dynamic  
107 settling tank receiving primary sludge and waste activated sludge before the AD,  
108 obtaining representative samples (30 L). At each sampling, the MS was characterized  
109 (see section 2.3) and stored at 4 °C. The inoculum employed for the start-up of the AD  
110 process was sampled from the digester operating at 37 °C in the same WWTP.

111 The biochar (Sewage Sludge - SS550a) considered in this work was selected among  
112 other BCs according to the results of previous studies as discussed in Section 2.2  
113 (Chiappero et al., 2021, Chiappero et al., *under review*). SS550 is a “standard” BC  
114 produced at the UK Biochar Research Centre (UKBRC) at the University of Edinburgh,  
115 UK (Mašek et al., 2018), through the slow pyrolysis of sewage sludge pellets at 550 °C  
116 in a continuously fed rotary kiln pyrolyzer (inner diameter 0.244 m, heated length 2.8  
117 m) with mean residence time of 30 min. Subsequently, the BC underwent physical  
118 activation with CO<sub>2</sub> at the Institute for Chemicals and Fuels from Alternative Resources  
119 (ICFAR) at Western University, Canada. Physical activation was performed in a  
120 horizontal 316 stainless steel tubular reactor 19 mm in diameter and 0.9 m long. The

121 biochar was placed between two stainless-steel woven mesh pads and the activation was  
122 carried out in a furnace at 900°C with a constant CO<sub>2</sub> flow rate of 200 mL/min and a  
123 holding time of 60 minutes. Therefore, the BC considered in this work was defined as  
124 “SS550a” (i.e., “SS550” according to the reference ID adopted at UKBRC, and “a” to  
125 refer to its activation).

126

## 127 *2.2. Semi-continuous anaerobic digestion test*

128 A lab-scale (3 L working volume) continuously stirred stainless-steel reactor (Methan  
129 Tube®, Biological Care, Italy) (Figure 1) was operated under a semi-continuous feeding  
130 mode for 100 days. The temperature was set to 37 °C (± 0.4 °C) and controlled through  
131 a built-in heater. Continuous mechanical mixing (75 rpm, reversed every 5 min) was  
132 provided by a brushless DC motor. For the start-up of the AD process, the digester was  
133 filled with digestate (see section 2.1), previously stored at 37 °C for 5 days. Once a day,  
134 at the same time after vigorous mixing, 0.150 L of MS at 3 % of TS load was manually  
135 fed to the reactor and 0.150 L of digestate automatically discharged, resulting in a  
136 hydraulic retention time (HRT) equal to 20 days and an OLR in the range 0.9-1.4 g<sub>VS</sub> L<sup>-1</sup>  
137 d<sup>-1</sup>. The AD tests involved two consequent phases. Phase 1 (control phase, CTRL):  
138 from day 0 to day 49, the digester was fed with MS. At day 31, a slight decrease of pH  
139 and total alkalinity was observed, thus the initial HRT equal to 15 days was adjusted to  
140 20 days. Phase 2: from day 50 to 100, 10 g L<sup>-1</sup> of BC was supplemented to the digester,  
141 feeding 1.5 g of BC and 0.150 mL of MS daily. This BC dose, recently used by other  
142 studies on the AD of wastewater sludge (Kaur et al., 2020; Liang et al., 2021; Wang et  
143 al., 2020) was selected based on the results of previous mesophilic AD batch tests  
144 performed on sludge sampled in the same WWTP and supplementing the same SS550s

145 BC, where it was found to enhance the methane yield from MS by 22 % (Chiappero et  
146 al., *under review*) and from waste activated sludge by 17 % (Chiappero et al., 2021), in  
147 order to investigate its effects on AD in semi-continuous feeding mode.

148

149 **Figure 1.** Configuration of the 3 L stainless-steel reactor: (1) motor and mixer; (2) gas  
150 outlet; (3) closing screws; (4) discharging port; (5) silicone stopper; (6) inflow; (7)  
151 heater connection; (8) outflow.

152

### 153 *2.3. Analytical procedures*

154 MS was characterized at every sampling (see section 2.1) and digestate was analysed  
155 every 3-4 days to monitor the key operating key parameters. pH and electrical  
156 conductivity (EC) were measured using a pH80+DHS (XS Instruments) multi-meter.  
157 Total solids (TS) and volatile solids (VS) were determined according to Standard  
158 Methods (APHA-AWWA-WEF, 2005). The total alkalinity (TA) was measured using  
159 the 2320B volumetric/potentiometric method (APHA-AWWA-WEF, 2005), on 40 mL  
160 of 1:10 diluted digestate titrated to pH 4.5 with 0.02 N hydrochloric acid. Total and  
161 soluble chemical oxygen demand (tCOD and sCOD), organic acids, and ammonia  
162 nitrogen were analyzed using Nanocolor test kits (Macherey-Nagel, Germany) and a  
163 PF-12<sup>Plus</sup> photometer (Macherey-Nagel, Germany). The samples were centrifuged  
164 (6,000 rpm for 10 min) and the supernatant used for ammonia nitrogen determination.  
165 The supernatant was filtered on 0.45 µm cellulose acetate membranes and analyzed for  
166 sCOD and organic acids. All analyses were carried out at least in duplicate.  
167 The parameters and analytical procedures involved in the characterization of the BC are  
168 detailed in the Appendix.



169 Biogas production was monitored daily through a gas flow meter ( $\mu$ Flow, Bioprocess  
170 Control, Sweden), automatically normalized to standard temperature and pressure (0 °C,  
171 1 atm). Biogas was collected in a 10 L gas sampling bag (30229-U, Supelco) and  
172 characterized (methane, carbon dioxide, hydrogen sulfide and oxygen) three times per  
173 week through an Optima 7 Biogas analyser (Mru GmbH, Germany).

174

#### 175 *2.4. Data analysis*

176 During the AD test, mean and standard error of the different parameters were  
177 determined for the time periods in which a constant organic loading rate (OLR) was fed  
178 to the digester. The relationship among BC addition, sludge characteristics and AD  
179 performances was assessed through single and multiple linear regression analyses.

180

#### 181 *2.5. Preliminary economic analysis*

182 A simplified economic analysis was carried out to estimate the maximum unit cost of  
183 BC (USD kg<sup>-1</sup>) that equals the higher revenues deriving from BC supplementation to the  
184 AD process. The input data of the AD process (Appendix) correspond to real tested  
185 conditions from the present study and recent literature, comparing five AD scenarios  
186 (PS, MS, food waste, and co-digestion of sewage sludge), where BC was supplemented  
187 to the continuous or semi-continuous digesters, at lab- or pilot-scale. Considering the  
188 costs, the simplified analysis was based exclusively on the cost of the BC; the capital  
189 costs and operational costs associated with the eventual improvement of the mixing  
190 inside the digester (due to the TS increase caused by BC) were not involved.

191 Considering the revenues, it was assumed that they derive from the “extra” (compared  
192 to the performances of AD without any supplement) energy obtained with BC addition,

193 with production of electrical energy in a combined heat and power (CHP) unit and  
194 supplying the thermal energy to the plant's energy needs. In details, the extra methane  
195 production was calculated as difference between the yield of BC amended reactors  
196 minus that of control reactors. The net economic profit was estimated given the methane  
197 lower heating value, the electrical energy efficiency of the CHP, and the average EU-27  
198 electricity price for non-household consumers (Appendix).

199

### 200 **3. Results and Discussion**

#### 201 *3.1. Characterization of substrate, inoculum, and biochar*

202 The average characteristics of the MS and of the inoculum are reported in Table 1. MS  
203 showed the typical characteristics of a mixed sludge (in average, pH 6.0 and TS 3.1%-  
204 wt). BC supplementation increased TS correspondingly to the dose of 10 g l<sup>-1</sup>, and  
205 reduced VS/TS due to the high ash content of the BC.

206

207 **Table 1.** Chemical characteristics of the mixed sludge, mixed sludge with 10 g L<sup>-1</sup> of  
208 SS550a biochar, and the digestate. Data are expressed as average ± standard error  
209 (number of values).

210

211 Considering the characteristics of the BC (see Appendix), the most significant are as  
212 follows. The specific surface area (109.2 m<sup>2</sup> g<sup>-1</sup>) and total pore volume (0.169 cm<sup>3</sup> g<sup>-1</sup>)  
213 are the result of the physical activation. The relevant ash content (58.9%-wt) and low  
214 total carbon (29.5%-wt) are expected based on the composition of the parent wastewater  
215 sludge (Metcalf & Eddy, 2013) from which the BC derives. The significant content of  
216 micro-elements contributed to the electrical conductivity (28 S m<sup>-1</sup>) and to the alkaline

217 pH (8.17). The main mineral constituents were Si, Al, Ca, S, P, K, present in the parent  
218 biomass and concentrated during the pyrolysis (Souza et al., 2021). Nutrients and alkali  
219 and alkaline earth metals are present in significant concentrations, compared to plant-  
220 based BCs (Qambrani et al., 2017). An adequate amount of alkali and alkaline earth  
221 metals in BC can contribute to the buffering capacity (Kaur et al., 2020). The H/C and  
222 O/C atomic ratios (respectively 0.54 and 0.17), indicate an intermediate hydrophobicity  
223 of the BC, in agreement with the literature (Zhang et al., 2020).

224

225 **Figure 2.** Biogas, methane, and carbon dioxide production during the semi-continuous  
226 AD of mixed sludge with and without BC: (A) Gas production as NmL d<sup>-1</sup>; (B) Gas  
227 production as NmL g tCOD<sup>-1</sup> d<sup>-1</sup>; (C) Gas production as NmL g v<sub>s</sub><sup>-1</sup> d<sup>-1</sup>; (D) CH<sub>4</sub>, CO<sub>2</sub>,  
228 and H<sub>2</sub>S concentration; (E) Organic loading rate as g<sub>vs</sub> L<sup>-1</sup> d<sup>-1</sup> and g tCOD L<sup>-1</sup> d<sup>-1</sup>.

229

### 230 3.2. Biogas and methane production

231 As detailed in section 2.2, the digester was fed for the first 50 days with MS (CTRL  
232 phase), and from day 51 to 100 supplementing 10 g l<sup>-1</sup> of BC. Figure 2 shows the  
233 production of biogas, methane and carbon dioxide, biogas composition and OLR during  
234 the different stages of the AD test. The MS was sampled four times during the test, and  
235 different physico-chemical features were observed (Table 1), thus the change of the  
236 substrate composition (specifically, VS/TS, tCOD and sCOD) and, consequently, of the  
237 organic loading rate (OLR) determined five constant sub-phases (Figure 2E): 1 to 3  
238 during CTRL phase, 4 and 5 during BC addition.

239

240 **Table 2.** Summary of the experimental results of the semi-continuous AD test, in each  
241 phase, reported as average (standard error).

242

243 The results of the AD test are detailed in Table 2. Daily biogas and methane yields  
244 (Figure 1A) reached stability around day 10, implying the conclusion of the start-up  
245 phase. Overall, during the experimental phase, biogas yield was in the range of 408-  
246 1120 NmL d<sup>-1</sup> and methane yield in the range of 315-724 NmL d<sup>-1</sup>. During the CTRL  
247 stage, biogas yield slightly decreased from phase 1 to 3 (from 791 ± 45 NmL d<sup>-1</sup> to 637  
248 ± 28 NmL d<sup>-1</sup>), and during phase 4 in the presence of BC (527 ± 18 NmL d<sup>-1</sup>) until day  
249 74, when a sharp increase occurred at the beginning of phase 5 (917 ± 26 NmL d<sup>-1</sup>).

250 Methane yield showed a similar trend, with a decline from a 525 ± 28 NmL d<sup>-1</sup> in phase  
251 1 during CTRL to 379 ± 19 NmL d<sup>-1</sup> in phase 4, followed by an increase to 636 ± 19  
252 NmL d<sup>-1</sup> in phase 5. It should be noticed that BC supplementation from day 50 did not  
253 seem to correspond to any variation of the decreasing trends observed for biogas and  
254 methane yields from phase 1 to 4. Conversely, the sharp increase at day 74 during the  
255 BC addition corresponded to a change in MS composition: sCOD of the MS was 1555 ±  
256 5 mg L<sup>-1</sup> in phase 1, 1123 ± 11 mg L<sup>-1</sup> in phase 2 and 3, 1870 ± 90 mg L<sup>-1</sup> in phase 4,  
257 and 3340 ± 30 mg L<sup>-1</sup> in phase 5.

258 The daily specific biogas and methane yields were also determined. The specific biogas  
259 yield (Figure 2B) decreased between phase 1 and 2 from 211 ± 12 to 163 ± 9 NmL g<sub>VS</sub><sup>-1</sup>  
260 d<sup>-1</sup>, then increased to 191 ± 9 NmL g<sub>VS</sub><sup>-1</sup> d<sup>-1</sup> (phase 3), remaining almost stable during  
261 phase 4, and finally jumped up to 286 ± 8 NmL g<sub>VS</sub><sup>-1</sup> d<sup>-1</sup> in phase 5. The specific  
262 methane yield followed a specular trend with a decrease between phases 1 and 2 (from

263  $140 \pm 7$  to  $113 \pm 7$  NmL g<sub>VS</sub><sup>-1</sup> d<sup>-1</sup>), followed by a slow rise (up to  $145 \pm 7$  NmL g<sub>VS</sub><sup>-1</sup> d<sup>-1</sup>)  
264 in phase 4 and a marked increase to  $198 \pm 6$  NmL g<sub>VS</sub><sup>-1</sup> d<sup>-1</sup> in phase 5.  
265 Similarly, specific biogas and methane yields expressed as NmL g<sub>tCOD</sub><sup>-1</sup> d<sup>-1</sup> (Figure 2C)  
266 confirmed the trends shown in Figure 2B, with minimum average values in phase 2 ( $92$   
267  $\pm 5$  and  $64 \pm 4$  NmL g<sub>tCOD</sub><sup>-1</sup> d<sup>-1</sup> respectively), and maximum values ( $157 \pm 4$  and  $109 \pm$   
268  $3$  NmL g<sub>tCOD</sub><sup>-1</sup> d<sup>-1</sup>) in phase 5. The addition of BC from day 50 did not correspond to  
269 any clear variation in specific biogas and methane yields between phases 3 and 4.  
270 Considering the biogas composition (Figure 2D), the stability of CH<sub>4</sub> and CO<sub>2</sub> contents  
271 over time was clear, in the range 67.1-69.0% and 28.6-30.8% during the CTRL phase,  
272 and 68.9-69.1 % and 29.6-30.1 % during BC addition, respectively. In all phases, the  
273 H<sub>2</sub>S concentration in biogas was almost negligible (below 16 ppm). Methane content of  
274 almost 70% confirmed a good stability of the AD process (Duan et al., 2012). However,  
275 under the specific experimental conditions, BC did not positively affect methane  
276 content, in contrast with literature. For instance, Shen et al. (2017) found an increase of  
277 14-25% of the average methane content with the addition of BCs derived from corn  
278 stover and pine, compared to a control reactor, during the temperature-phased semi-  
279 continuous AD of sludge at 55 °C. Wei et al. (2020) showed that supplementation of  
280 corn stover BC enhanced methane content up to 21% compared to control reactors  
281 during the continuous AD of primary sludge at 55 °C.  
282 Figure 2E shows the trend of the OLR, expressed as VS and tCOD (as commonly found  
283 in literature), during the AD test. In general, OLR did not vary significantly over the  
284 duration of the test, ranging between 0.9-1.4 g<sub>VS</sub> L<sup>-1</sup>d<sup>-1</sup> and 1.6-2.1 g<sub>tCOD</sub> L<sup>-1</sup>d<sup>-1</sup>,  
285 which are typical values adopted in full-scale mesophilic digesters in WWTPs  
286 (Bolzonella et al., 2005). However, OLR did not seem to positively affect the specific

287 biogas and methane yields observed in this work. In phase 2, the highest OLR values  
288 (1.4 g<sub>VS</sub> L<sup>-1</sup>d<sup>-1</sup>, 2.1 g tCOD L<sup>-1</sup>d<sup>-1</sup>) corresponded to the minimum specific biogas and  
289 methane yields, equal to 163 ± 9 and 113 ± 7 NmL g<sub>VS</sub><sup>-1</sup>d<sup>-1</sup>, respectively. More  
290 importantly, the marked increase in specific biogas (+42%) and methane yields (+37%)  
291 between phases 4 and 5 did not match a pronounced variation of the OLR.

292

293 **Table 3.** Results of multiple linear regression to predict biogas and anaerobic digestate  
294 parameters based on OLR as sCOD (g sCOD L<sup>-1</sup> d<sup>-1</sup>) and BC concentration (g L<sup>-1</sup>). The  
295 linear model is expressed in the form  $y = b_0 + b_1 x_1 + b_2 x_2$ , where  $y$  is the estimated  
296 parameter,  $x_1$  is the OLR,  $x_2$  is BC concentration.

297

298 In parallel to the usual notations applied to OLR (expressed as VS and tCOD), we  
299 decided to investigate the influence of sCOD on the OLR and included it in the further  
300 evaluation of our experimental results. The soluble COD represents the fraction of COD  
301 immediately accessible by microorganisms for degradation. The ratio between sCOD  
302 and tCOD is used to quantify the degree of solubilization of the sludge, usually  
303 considered as performance indicator to investigate the efficiency of pre-treatments in  
304 improving the methane yield (Nguyen et al., 2021). In this study, despite the stability of  
305 TS content (around 3.1%), the MS presented a variable sCOD/tCOD, in the range 2.9 –  
306 8.6% (Figure 2E).

307 Since the increment in the methane yields during the BC addition occurred concurrently  
308 with a change in MS composition, a single linear regression was used to investigate the  
309 relationships between the specific biogas and methane yields (NmL kg<sub>VS</sub><sup>-1</sup>d<sup>-1</sup>) and the  
310 key characteristics of the MS, namely the OLR (expressed as VS, tCOD and sCOD),

311 and the sCOD/tCOD (%). A significant linear relation was not identified between the  
312 specific biogas yield and the OLR expressed as  $\text{g VS L}^{-1} \text{d}^{-1}$  ( $F(1.63) = 3.48, p > 0.05$ ) or  
313 as  $\text{g tCOD L}^{-1} \text{d}^{-1}$  ( $F(1.63) = 2.56, p > 0.05$ ). Conversely, a significant positive linear  
314 relation was found between biogas yield and the OLR expressed as  $\text{g sCOD L}^{-1} \text{d}^{-1}$   
315 ( $F(1.63) = 102.38, p = 7.9 \text{ e-}15$ ) with an  $R^2$  of 0.60, and between the biogas yield and  
316 the sCOD/tCOD (%) ( $F(1.63) = 93.87, p = 4.2 \text{ e-}14$ ) with an  $R^2$  of 0.62. As for biogas,  
317 significant linear relationships between the specific methane yield expressed as  $\text{NmL}$   
318  $\text{kgVS}^{-1}\text{d}^{-1}$  and the OLR expressed as VS ( $F(1.37) = 3.56, p > 0.05$ ) or as tCOD ( $F(1.37) =$   
319  $2.47, p > 0.05$ ) were not found. In contrast, a significant positive linear relationship was  
320 identified for methane yield and OLR expressed as sCOD with an  $R^2$  of 0.67 ( $F(1.37) =$   
321  $75.41, p = 1.9 \text{ e-}10$ ) and methane yield and sCOD/tCOD (%) with an  $R^2$  of 0.68  
322 ( $F(1.63) = 79.17, p = 1.0 \text{ e-}10$ ). Therefore, the marked increase of the specific biogas  
323 and methane yields in phase 5 may be ascribable to the corresponding increase of  
324 sCOD/tCOD (%) in the MS from 5.8 % of phase 4 to 8.6 % of phase 5 (Figure 2E).  
325 Given the significant role of MS composition (specifically, sCOD content) on biogas  
326 and methane productions, the relative effect of BC addition and MS features on biogas  
327 production and composition was further investigated through a multiple linear  
328 regression analysis. From the results of the simple linear regression analysis, OLR  
329 expressed as sCOD was identified as the most appropriate parameter to describe the MS  
330 composition. Two independent variables, namely OLR expressed as  $\text{g sCOD L}^{-1} \text{d}^{-1}$  and  
331 BC concentration ( $\text{g L}^{-1}$ ) were chosen to predict biogas and methane yields, and biogas  
332 composition. The linear model was expressed in the form  $y = b_0 + b_1 x_1 + b_2 x_2$ , where  $y$   
333 is the estimated parameter,  $x_1$  is the OLR,  $x_2$  is the BC concentration. Considering the  
334 results of the multiple linear regression analysis (Table 3), in general, the linear

335 regressions for daily biogas and methane yields ( $\text{NmL d}^{-1}$ ) were significant, with  $R^2$   
336 equal to 0.69 and 0.73, respectively. While significant positive relationships ( $b_1 > 0$ ,  
337  $p_1 < 0.05$ ) for biogas or methane yields and OLR were confirmed, there were significant  
338 negative relationships ( $b_2 < 0$ ,  $p_2 < 0.05$ ) with BC concentration. Further, positive linear  
339 regressions were found between the specific biogas and methane yields ( $\text{NmL gVS}^{-1} \text{d}^{-1}$ )  
340 and the OLR. However, there was insufficient evidence ( $p_2 > 0.05$ ) to conclude that  
341 specific biogas and methane yields were positively ( $b_2 > 0$ ) affected by BC  
342 supplementation. As expected, the linear regressions of  $\text{CH}_4$  and  $\text{CO}_2$  contents based on  
343 OLR expressed as sCOD and BC concentration did not show any relationship.  
344 Conversely, other studies proved that BC supplementation can enhance methane  
345 production from sludge during continuous AD, adopting different operating conditions  
346 or BC dosage and characteristics, compared to this work. As mentioned earlier, Shen et  
347 al. (2017) demonstrated the enhancement of methane production from two-stage AD of  
348 mixed sludge at  $55^\circ\text{C}$  with the addition of corn stover BC. In that study, the positive  
349 effects of BC were attributed to  $\text{CO}_2$  removal, mitigation of ammonia inhibition,  
350 increased alkalinity, shifts of microbial community, and linked to peculiar BC features  
351 as the large specific surface area and micro-porous structure, high hydrophobicity and  
352 content of aromatics and alkali and alkaline earth metals. Also Wei et al. (2020), testing  
353 a BC having similar characteristics than the one considered by Shen et al. (2017), found  
354 that BC increased methane production during thermophilic AD of primary sludge;  
355 enhanced buffering capacity, alleviated ammonia inhibition, and  $\text{CO}_2$  sequestration  
356 were suggested as main mechanisms. Compared to the BCs used in the two mentioned  
357 studies, SS550a presents comparable specific surface area ( $109.2 \text{ m}^2 \text{ g}^{-1}$ ), micro-porous  
358 structure (total pore volume  $0.169 \text{ cm}^3 \text{ g}^{-1}$ , 6.19 average pore diameter), and contents of



359 alkali and alkaline earth metals, but also a less alkaline pH, lower hydrophobicity, and  
360 higher H/C and O/C ratios. However, the main difference in the BC, compared with the  
361 two cited studies, may consist in the lower dosage of BC adopted in the present work,  
362 equal to 10 g L<sup>-1</sup> of BC (corresponding to 0.50 ± 0.03 g BC/g<sub>VS</sub> added, and 0.32 ± 0.01  
363 g BC/g<sub>TS</sub>), being 3.5-7 times lower than those of the other studies, with an optimum of  
364 1.75-3.5 g BC/g<sub>VS</sub> (Shen et al., 2017) and 1.82 g BC/g<sub>TS</sub> (Wei et al., 2020). Moreover,  
365 the cited studies fed the same substrate during the whole duration of their AD tests,  
366 therefore the influence of the variability of sludge composition on the performance of  
367 the AD in the presence of BC, which was highlighted as a key issue by the results of  
368 this work, was not specifically explored in the literature.

369

370 **Figure 3.** Characteristics of the digestate during the AD test: (A) total and soluble  
371 COD; (B) Total Solids and Volatile Solids; (C) Removals of total COD and soluble  
372 COD; (D) Removals of Total Solids and Volatile Solids; (E) pH and Electrical  
373 Conductivity; (F) Total Alkalinity, Organic Acids, Ammonia Nitrogen.

374

### 375 *3.3. Digestate characterization*

376 The trends of the characteristics of the digestate (Figure 3A) show that tCOD grew  
377 during phase 1, then stabilized during the subsequent phases at 30-32 g L<sup>-1</sup> (Table 2).  
378 The stabilization of tCOD from the start-up phase was slower than that of the biogas  
379 and methane yields. The sCOD remained relatively stable, below 860 mg L<sup>-1</sup>, with  
380 average values ranged between 540 and 730 mg L<sup>-1</sup> during the different phases of the  
381 test (Figure 3A). The linear relationships between output tCOD or sCOD and BC  
382 concentration and OLR (expressed as sCOD) were not significant (Table 3).

383 The TS concentration (Figure 3B) was relatively stable during CTRL phase, with  
384 average values in the range 2.92-3.25%, and slowly increased from day 50. Conversely,  
385 the VS concentration remained relatively stable at 1.64-1.91% during the whole test.  
386 The VS/TS ratio decreased from 56.3-57.3 % in the CTRL phase to 52.8-53.2 % with  
387 the BC addition (Table 2). The results of the multiple linear regression analysis showed  
388 a significant positive relationship between BC concentration and TS content, along with  
389 a significant negative relationship between BC and VS/TS (Table 3). Obviously, OLR  
390 expressed as sCOD did not significantly influence the TS and VS/TS ratio.  
391 Despite the variability of sCOD in the input, the AD system reached a stable  
392 concentration in the output. Overall, the resulting removals of tCOD and sCOD over  
393 time were consistent with the biogas and methane yields (Figure 3C). The trend of  
394 tCOD removal decreased from the initial values of phase 1 in the CTRL phase to  
395 minimum values in phase 4, followed by an increase from day 70 up to an average of  $32$   
396  $\pm 3$  % (Table 2) in phase 5. The obtained tCOD removal values in phase 5 (Table 2) are  
397 consistent with literature, where tCOD removals are in the range 34-55 % (Astals et al.,  
398 2012; Choi et al., 2018; Hidaka et al., 2013). Consistently with the trend of specific  
399 methane yield, sCOD removal (Figure 3C) showed a decline from a mean of  $65 \pm 8$  %  
400 of phase 1 to  $35 \pm 4$  % of phase 3, rising to  $80 \pm 2$  % in phase 5. As for biogas and  
401 methane yields, the multiple linear regression analysis found significant positive  
402 relationships ( $b_1 > 0$ ,  $p_1 < 0.05$ ) for the removals of tCOD or sCOD and OLR as sCOD,  
403 due to the relative stability of the output concentrations and the variability of sCOD in  
404 the feed. Conversely, there was no evidence of positive effects of the BC  
405 supplementation on COD removal.

406 The removal of TS and of VS (Figure 3D) were in the range 3.8-10.4% and 9.6-22.1%  
407 in the CTRL phase, respectively, and in the range 4.5-32.5 % and 3.9-31.3 % with BC  
408 supplementation. The multiple linear regression analysis did not find significant linear  
409 relationships between solids removals and predictor variables (Table 3). Consistently  
410 with biogas and methane productions, BC was not found to enhance the removal of  
411 organic matter during the mesophilic semi-continuous AD of mixed sludge. These  
412 results differ from those of Wei et al. (2020) who found an increase of 14.9% of VS  
413 removal in presence of BC, compared to the control reactor, during the continuous AD  
414 of primary sludge.

415 The pH was stable during the whole AD tests around 6.9-7.2 (Figure 3E), in the optimal  
416 range for methanogens (Xu et al., 2020) and indicating a good process stability. The  
417 Electrical Conductivity (EC) of the digestate ranged between 4.1 and 5.7 mS cm<sup>-1</sup>,  
418 showing the highest values in phase 5 (5.1 ± 0.1 mS cm<sup>-1</sup>). However, there was no  
419 evidence of a significant positive effect of the BC concentration on the EC of the  
420 digestate (Table 3), despite the relevant contents of cations in the BC (Table 2).

421 Figure 3F shows the trends of total alkalinity (TA), organic acids and ammonia nitrogen  
422 concentrations in the digestate. Organic acids are important intermediates in the AD  
423 processes, converted to carbon dioxide and methane by syntrophic acetogens and  
424 methanogens, can accumulate with potential inhibitory effects on methanogens. The  
425 total alkalinity is an indicator of the buffering capacity of the system, e.g. of the ability  
426 of neutralizing organic acids. This is the reason why the control of total alkalinity and  
427 organic acids concentrations is crucial for the stability of any AD system. TA ranged  
428 from 2700 to 2900 mg l<sup>-1</sup> CaCO<sub>3</sub> during CTRL phase, and from 3000 to 3300 mg l<sup>-1</sup>  
429 CaCO<sub>3</sub> with BC addition. Multiple linear regression analysis found a significant

430 positive relationship between BC concentration and TA in the digestate ( $b_2 > 0$ ,  $p_2 < 0.05$ ),  
431 possibly related to a BC contribution to the buffering capacity of the system. The TA  
432 increase is related to the alkalinity of SS550a BC, due to the presence of high contents  
433 of K, Ca, Mg, Al in the ashes, as reported by other studies (Shen et al., 2015; Wang et  
434 al., 2017; Zhou et al., 2020). The organic acids in the digestate were relatively stable  
435 below concentrations of concern, with average values ranging 117-233 mg l<sup>-1</sup> of acetic  
436 acid. Despite the variability of sCOD in input, there was not a significant effect of OLR  
437 expressed as sCOD on the concentration of organic acids in output (Table 3),  
438 consistently with previous results related to sCOD in the digestate. Further, the ratio  
439 between organic acids and TA was relatively stable between 0.03 and 0.09. A ratio  
440 below 0.4 is generally recommended for stable AD operations (Ahmed et al., 2021;  
441 Zhou et al., 2020). Ammonia nitrogen concentration in the digestate (Figure 3F)  
442 remained relatively stable around 400-600 mg l<sup>-1</sup>, below inhibitory concentrations for  
443 the AD process (Jiang et al., 2019). There was no evidence of a significant relationship  
444 between BC concentration and ammonia nitrogen in the digestate from the multiple  
445 linear regression analysis. Instead, other studies found a reduction of ammonia nitrogen  
446 in presence of BC (Shen et al., 2015; Zhang et al., 2019). Ammonia nitrogen, produced  
447 during AD through ammonification, could further contribute to the buffering capacity of  
448 AD system. A significant positive relationship ( $F(1,20) = 30.70$ ,  $p = 2e-5$ ,  $R^2 0.61$ )  
449 between Ammonia nitrogen and TA was found by the multiple linear regression of the  
450 experimental data of this work.

451

452 *3.4. Preliminary economic analysis*

453 The key question is whether the economic benefits deriving from BC addition exceed its  
454 cost. The main benefit is the extra (compared to AD without any supplement) methane  
455 yield, resulting in higher incomes from the sale of electricity. However, extra costs  
456 derive from the supplementation of BC. A simplified economic analysis (section 2.5)  
457 estimated the maximum unit cost of BC that equals the profits from the enhanced  
458 methane yield in different scenarios. In this study (semi-continuous AD of MS at 37  
459 °C), an enhanced methane yield of 22 % due to a dose of 10 g L<sup>-1</sup> could be cost-  
460 effective with a unit cost of BC below 0.043 USD kg<sup>-1</sup>. This value is borderline with  
461 respect of a typical range cost for BC of 0.05 - 0.5 USD kg<sup>-1</sup> (Chiappero et al., 2020;  
462 Chiappero et al., under review). Other studies presented different results (see Appendix)  
463 depending on OLR, enhancement of methane yield, and BC dose. For instance, values  
464 ranging 0.017-0.022 USD kg<sup>-1</sup> were found for the AD of MS, due to similar  
465 enhancements of methane yield (+ 21-27 %) but larger doses of BC (18.75 g L<sup>-1</sup>).  
466 Conversely, the AD of PS resulted in a higher maximum unit cost of 0.184 USD kg<sup>-1</sup>,  
467 due to the larger OLR and the lower dose of BC. Further, promising results were  
468 obtained for other scenarios regarding the AD of food waste and co-digestion of sewage  
469 sludge and orange peel with maximum BC unit costs of 0.329 and 0.524 USD kg<sup>-1</sup>,  
470 respectively, where the authors found larger improvements of CH<sub>4</sub> yields (38 % and 61  
471 %) by adding similar doses of BC (15 and 10 g L<sup>-1</sup>). Overall, the optimization of BC  
472 dosage may be a key step towards the economic feasibility of BC supplementation in  
473 AD.

474

#### 475 **4. Conclusions**

476 This research proved that, under the considered experimental conditions, the sCOD of  
477 the substrate was the driving factor for the performances of the AD of MS,  
478 independently of BC addition. This happens particularly in the AD of MS (because of  
479 the high variability of the quality of PS), compared to the digestion of WAS, whose  
480 composition is less variable. The same BC, tested in batch AD of sludge from the same  
481 WWTP, was able to improve of 17% the methane yields obtained from WAS  
482 (Chiappero et al., 2021) and of 22% from MS (Chiappero et al. under review).

483

#### 484 **Acknowledgements**

485 This research was funded with internal resources. The authors declare no conflict of  
486 interest. The authors would like to thank CORDAR Biella Servizi SpA for supplying  
487 the substrate and inoculum employed in this research. Authors' contributions:  
488 experimental activity, data elaboration, original draft writing: M. Chiappero;  
489 conceptualization, methodology, supervision, original draft writing: S. Fiore;  
490 manuscript review: all authors.

491

#### 492 **References**

- 493 1. Abbas, Y., Yun, S., Wang, Z., Zhang, Y., Zhang, X., Wang, K., 2021. Recent  
494 advances in bio-based carbon materials for anaerobic digestion: A review. *Renew.*  
495 *Sustain. Energy Rev.* <https://doi.org/10.1016/j.rser.2020.110378>
- 496 2. Ahmed, M., Sartori, F., Merzari, F., Fiori, L., Elagroudy, S., Negm, M.S.,  
497 Andreottola, G., 2021. Anaerobic degradation of digestate based hydrothermal  
498 carbonization products in a continuous hybrid fixed bed anaerobic filter. *Bioresour.*  
499 *Technol.* 330, 124971. <https://doi.org/10.1016/J.BIORTECH.2021.124971>
- 500 3. Alenzi, A., Hunter, C., Spencer, J., Roberts, J., Craft, J., Pahl, O., Escudero, A.,  
501 2021. Pharmaceuticals effect and removal, at environmentally relevant

- 502 concentrations, from sewage sludge during anaerobic digestion. *Bioresour.*  
503 *Technol.* 319, 124102. <https://doi.org/10.1016/J.BIORTECH.2020.124102>
- 504 4. APHA-AWWA-WEF, 2005. *Standard methods for the examination of water and*  
505 *wastewater*, 21st ed. Washington, DC, US.
- 506 5. Appels, L., Degrève, J., Van der Bruggen, B., Van Impe, J., Dewil, R., 2010.  
507 *Influence of low temperature thermal pre-treatment on sludge solubilisation, heavy*  
508 *metal release and anaerobic digestion.* *Bioresour. Technol.* 101, 5743–5748.  
509 <https://doi.org/10.1016/j.biortech.2010.02.068>
- 510 6. Astals, S., Venegas, C., Peces, M., Jofre, J., Lucena, F., Mata-Alvarez, J., 2012.  
511 *Balancing hygienization and anaerobic digestion of raw sewage sludge.* *Water Res.*  
512 46, 6218–6227. <https://doi.org/10.1016/J.WATRES.2012.07.035>
- 513 7. Bolzonella, D., Pavan, P., Battistoni, P., Cecchi, F., 2005. *Mesophilic anaerobic*  
514 *digestion of waste activated sludge: Influence of the solid retention time in the*  
515 *wastewater treatment process.* *Process Biochem.* 40, 1453–1460.  
516 <https://doi.org/10.1016/j.procbio.2004.06.036>
- 517 8. Chiappero, M., Berruti, F., Mašek, O., Fiore, S., 2021. *Analysis of the influence of*  
518 *activated biochar properties on methane production from anaerobic digestion of*  
519 *waste activated sludge.* *Biomass and Bioenergy* 150, 106129.  
520 <https://doi.org/10.1016/j.biombioe.2021.106129>
- 521 9. Chiappero, M., Cillerai, F., Berruti, F., Mašek, O., Fiore, S., n.d. *Addition of*  
522 *different biochars as catalysts during the mesophilic anaerobic digestion of mixed*  
523 *sludge.* *Catalysts* (under review).
- 524 10. Chiappero, M., Norouzi, O., Hu, M., Demichelis, F., Berruti, F., Di Maria, F.,  
525 Mašek, O., Fiore, S., 2020. *Review of biochar role as additive in anaerobic*  
526 *digestion processes.* *Renew. Sustain. Energy Rev.* 131.  
527 <https://doi.org/10.1016/j.rser.2020.110037>
- 528 11. Choi, J.M., Han, S.K., Lee, C.Y., 2018. *Enhancement of methane production in*  
529 *anaerobic digestion of sewage sludge by thermal hydrolysis pretreatment.*  
530 *Bioresour. Technol.* 259, 207–213.  
531 <https://doi.org/10.1016/J.BIORTECH.2018.02.123>
- 532 12. Duan, N., Dong, B., Wu, B., Dai, X., 2012. *High-solid anaerobic digestion of*  
533 *sewage sludge under mesophilic conditions: Feasibility study.* *Bioresour. Technol.*

- 534 104, 150–156. <https://doi.org/10.1016/j.biortech.2011.10.090>
- 535 13. Elalami, D., Carrere, H., Monlau, F., Abdelouahdi, K., Oukarroum, A., Barakat, A.,  
536 2019. Pretreatment and co-digestion of wastewater sludge for biogas production:  
537 Recent research advances and trends. *Renew. Sustain. Energy Rev.* 114, 109287.  
538 <https://doi.org/10.1016/j.rser.2019.109287>
- 539 14. Eurostat, 2021. Sewage sludge production and disposal [WWW Document]. URL  
540 [https://appsso.eurostat.ec.europa.eu/nui/show.do?dataset=env\\_ww\\_spd&lang=en](https://appsso.eurostat.ec.europa.eu/nui/show.do?dataset=env_ww_spd&lang=en)  
541 (accessed 3.9.21).
- 542 15. Gherghel, A., Teodosiu, C., De Gisi, S., 2019. A review on wastewater sludge  
543 valorisation and its challenges in the context of circular economy. *J. Clean. Prod.*  
544 <https://doi.org/10.1016/j.jclepro.2019.04.240>
- 545 16. Gu, Y., Li, Y., Li, X., Luo, P., Wang, H., Wang, X., Wu, J., Li, F., 2017. Energy  
546 self-sufficient wastewater treatment plants: Feasibilities and challenges, in: *Energy*  
547 *Procedia*. Elsevier Ltd, pp. 3741–3751.  
548 <https://doi.org/10.1016/j.egypro.2017.03.868>
- 549 17. Hidaka, T., Wang, F., Togari, T., Uchida, T., Suzuki, Y., 2013. Comparative  
550 performance of mesophilic and thermophilic anaerobic digestion for high-solid  
551 sewage sludge. *Bioresour. Technol.* 149, 177–183.  
552 <https://doi.org/10.1016/J.BIORTECH.2013.09.033>
- 553 18. Jenicek, P., Kutil, J., Benes, O., Todt, V., Zabranska, J., Dohanyos, M., 2013.  
554 Energy self-sufficient sewage wastewater treatment plants: Is optimized anaerobic  
555 sludge digestion the key? *Water Sci. Technol.* 68, 1739–1743.  
556 <https://doi.org/10.2166/wst.2013.423>
- 557 19. Jiang, Y., McAdam, E., Zhang, Y., Heaven, S., Banks, C., Longhurst, P., 2019.  
558 Ammonia inhibition and toxicity in anaerobic digestion: A critical review. *J. Water*  
559 *Process Eng.* 32, 100899. <https://doi.org/10.1016/J.JWPE.2019.100899>
- 560 20. Kaur, G., Johnravindar, D., Wong, J.W.C., 2020. Enhanced volatile fatty acid  
561 degradation and methane production efficiency by biochar addition in food waste-  
562 sludge co-digestion: A step towards increased organic loading efficiency in co-  
563 digestion. *Bioresour. Technol.* 308, 123250.  
564 <https://doi.org/10.1016/j.biortech.2020.123250>
- 565 21. Khanh Nguyen, V., Kumar Chaudhary, D., Hari Dahal, R., Hoang Trinh, N., Kim,



- 566 J., Chang, S.W., Hong, Y., Duc La, D., Nguyen, X.C., Hao Ngo, H., Chung, W.J.,  
567 Nguyen, D.D., 2021. Review on pretreatment techniques to improve anaerobic  
568 digestion of sewage sludge. *Fuel* 285, 119105.  
569 <https://doi.org/10.1016/j.fuel.2020.119105>
- 570 22. Li, S., Harris, S., Anandhi, A., Chen, G., 2019. Predicting biochar properties and  
571 functions based on feedstock and pyrolysis temperature: A review and data  
572 syntheses. *J. Clean. Prod.* 215, 890–902.  
573 <https://doi.org/10.1016/j.jclepro.2019.01.106>
- 574 23. Liang, J., Luo, L., Li, D., Varjani, S., Xu, Y., Wong, J.W.C., 2021. Promoting  
575 anaerobic co-digestion of sewage sludge and food waste with different types of  
576 conductive materials: Performance, stability, and underlying mechanism.  
577 *Bioresour. Technol.* 337, 125384. <https://doi.org/10.1016/j.biortech.2021.125384>
- 578 24. Lü, C., Shen, Y., Li, C., Zhu, N., Yuan, H., 2020. Redox-active biochar and  
579 conductive graphite stimulate methanogenic metabolism in anaerobic digestion of  
580 waste-activated sludge: Beyond direct interspecies electron transfer. *ACS Sustain.*  
581 *Chem. Eng.* 8, 12626–12636. <https://doi.org/10.1021/acssuschemeng.0c04109>
- 582 25. Lu, J.S., Chang, J.S., Lee, D.J., 2020. Adding carbon-based materials on anaerobic  
583 digestion performance: A mini-review. *Bioresour. Technol.* 300, 122696.  
584 <https://doi.org/10.1016/j.biortech.2019.122696>
- 585 26. Mašek, O., Buss, W., Roy-Poirier, A., Lowe, W., Peters, C., Brownsort, P.,  
586 Mignard, D., Pritchard, C., Sohi, S., 2018. Consistency of biochar properties over  
587 time and production scales: A characterisation of standard materials. *J. Anal. Appl.*  
588 *Pyrolysis* 132, 200–210. <https://doi.org/10.1016/j.jaap.2018.02.020>
- 589 27. Metcalf & Eddy, Tchobanoglous, G., Stensel, H.D., Tsuchihashi, R., Burton, F.,  
590 2013. *Wastewater Engineering: Treatment and Resource Recovery*, 5th ed.  
591 McGraw-Hill Education, New York, NY.
- 592 28. Mohammad Mirsoleimani Azizi, S., Hai, F.I., Lu, W., Al-Mamun, A., Ranjan Dhar,  
593 B., 2021. A review of mechanisms underlying the impacts of (nano)microplastics  
594 on anaerobic digestion. *Bioresour. Technol.* 329, 124894.  
595 <https://doi.org/10.1016/J.BIORTECH.2021.124894>
- 596 29. Panepinto, D., Fiore, S., Genon, G., Acri, M., 2016. Thermal valorization of sewer  
597 sludge: Perspectives for large wastewater treatment plants. *J. Clean. Prod.* 137,

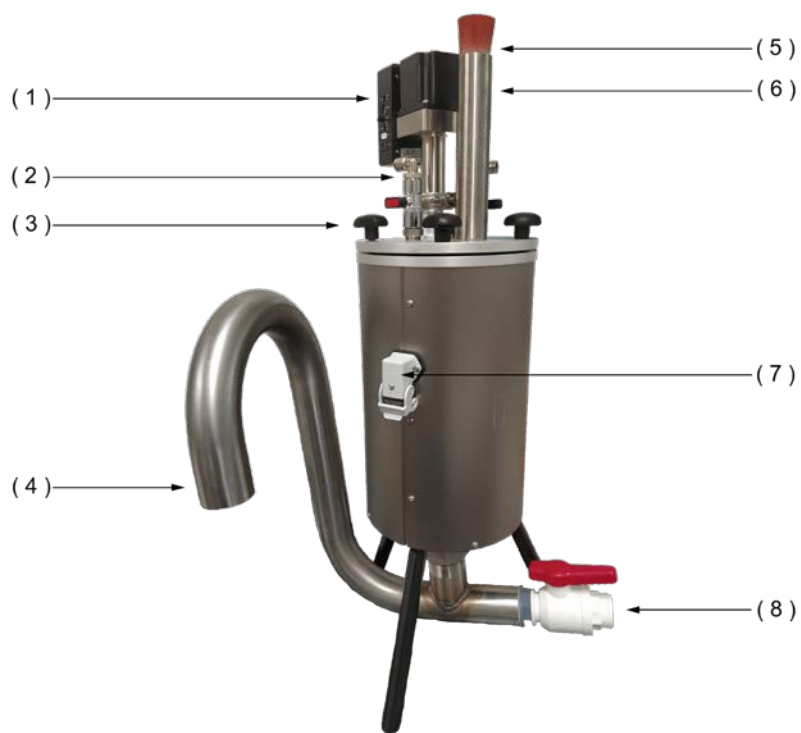
- 598 1323–1329. <https://doi.org/10.1016/j.jclepro.2016.08.014>
- 599 30. Qambrani, N.A., Rahman, M.M., Won, S., Shim, S., Ra, C., 2017. Biochar  
600 properties and eco-friendly applications for climate change mitigation, waste  
601 management, and wastewater treatment: A review. *Renew. Sustain. Energy Rev.*  
602 79, 255–273. <https://doi.org/10.1016/j.rser.2017.05.057>
- 603 31. Shen, Y., Forrester, S., Koval, J., Urgan-Demirtas, M., 2017. Yearlong semi-  
604 continuous operation of thermophilic two-stage anaerobic digesters amended with  
605 biochar for enhanced biomethane production. *J. Clean. Prod.* 167, 863–874.  
606 <https://doi.org/10.1016/j.jclepro.2017.05.135>
- 607 32. Shen, Y., Linville, J.L., Ignacio-de Leon, P.A.A., Schoene, R.P., Urgan-Demirtas,  
608 M., 2016. Towards a sustainable paradigm of waste-to-energy process: Enhanced  
609 anaerobic digestion of sludge with woody biochar. *J. Clean. Prod.* 135, 1054–1064.  
610 <https://doi.org/10.1016/j.jclepro.2016.06.144>
- 611 33. Shen, Y., Linville, J.L., Urgan-Demirtas, M., Schoene, R.P., Snyder, S.W., 2015.  
612 Producing pipeline-quality biomethane via anaerobic digestion of sludge amended  
613 with corn stover biochar with in-situ CO<sub>2</sub> removal. *Appl. Energy* 158, 300–309.  
614 <https://doi.org/10.1016/j.apenergy.2015.08.016>
- 615 34. Shen, Y., Yu, Y., Zhang, Y., Urgan-Demirtas, M., Yuan, H., Zhu, N., Dai, X.,  
616 2021. Role of redox-active biochar with distinctive electrochemical properties to  
617 promote methane production in anaerobic digestion of waste activated sludge. *J.*  
618 *Clean. Prod.* 278, 123212. <https://doi.org/10.1016/j.jclepro.2020.123212>
- 619 35. Souza, C. de S., Bomfim, M.R., Almeida, M. da C. de, Alves, L. de S., Santana,  
620 W.N. de, Amorim, I.C. da S., Santos, J.A.G., 2021. Induced changes of pyrolysis  
621 temperature on the physicochemical traits of sewage sludge and on the potential  
622 ecological risks. *Sci. Reports* 2021 11, 1–13. [https://doi.org/10.1038/s41598-](https://doi.org/10.1038/s41598-020-79658-4)  
623 [020-79658-4](https://doi.org/10.1038/s41598-020-79658-4)
- 624 36. Wang, D., Ai, J., Shen, F., Yang, G., Zhang, Y., Deng, S., Zhang, J., Zeng, Y.,  
625 Song, C., 2017. Improving anaerobic digestion of easy-acidification substrates by  
626 promoting buffering capacity using biochar derived from vermicompost. *Bioresour.*  
627 *Technol.* 227, 286–296. <https://doi.org/10.1016/j.biortech.2016.12.060>
- 628 37. Wang, P., Peng, H., Adhikari, S., Higgins, B., Roy, P., Dai, W., Shi, X., 2020.  
629 Enhancement of biogas production from wastewater sludge via anaerobic digestion

- 630 assisted with biochar amendment. *Bioresour. Technol.* 309.  
631 <https://doi.org/10.1016/j.biortech.2020.123368>
- 632 38. Wei, W., Guo, W., Ngo, H.H., Mannina, G., Wang, D., Chen, X., Liu, Y., Peng, L.,  
633 Ni, B.-J., 2020. Enhanced high-quality biomethane production from anaerobic  
634 digestion of primary sludge by corn stover biochar. *Bioresour. Technol.* 306.  
635 <https://doi.org/10.1016/j.biortech.2020.123159>
- 636 39. Wu, B., Yang, Q., Yao, F., Chen, S., He, L., Hou, K., Pi, Z., Yin, H., Fu, J., Wang,  
637 D., Wang, D., Li, X., 2019. Evaluating the effect of biochar on mesophilic  
638 anaerobic digestion of waste activated sludge and microbial diversity. *Bioresour.*  
639 *Technol.* 294. <https://doi.org/10.1016/j.biortech.2019.122235>
- 640 40. Xu, H., Li, Y., Hua, D., Zhao, Y., Mu, H., Chen, H., Chen, G., 2020. Enhancing the  
641 anaerobic digestion of corn stover by chemical pretreatment with the black liquor  
642 from the paper industry. *Bioresour. Technol.* 306, 123090.  
643 <https://doi.org/10.1016/J.BIORTECH.2020.123090>
- 644 41. Xu, S., Wang, C., Duan, Y., Wong, J.W.C., 2020. Impact of pyrochar and  
645 hydrochar derived from digestate on the co-digestion of sewage sludge and swine  
646 manure. *Bioresour. Technol.* 314, 123730.  
647 <https://doi.org/10.1016/j.biortech.2020.123730>
- 648 42. Yin, C., Shen, Y., Yuan, R., Zhu, N., Yuan, H., Lou, Z., 2019. Sludge-based  
649 biochar-assisted thermophilic anaerobic digestion of waste-activated sludge in  
650 microbial electrolysis cell for methane production. *Bioresour. Technol.* 284, 315–  
651 324. <https://doi.org/10.1016/j.biortech.2019.03.146>
- 652 43. Zhang, M., Li, J., Wang, Y., Yang, C., 2019. Impacts of different biochar types on  
653 the anaerobic digestion of sewage sludge. *RSC Adv.* 9, 42375–42386.  
654 <https://doi.org/10.1039/c9ra08700a>
- 655 44. Zhang, M., Wang, Y., 2020. Effects of Fe-Mn-modified biochar addition on  
656 anaerobic digestion of sewage sludge: Biomethane production, heavy metal  
657 speciation and performance stability. *Bioresour. Technol.* 313.  
658 <https://doi.org/10.1016/j.biortech.2020.123695>
- 659 45. Zhang, P., Zhang, X., Li, Y., Han, L., 2020. Influence of pyrolysis temperature on  
660 chemical speciation, leaching ability, and environmental risk of heavy metals in  
661 biochar derived from cow manure. *Bioresour. Technol.* 302, 122850.

- 662 <https://doi.org/10.1016/J.BIORTECH.2020.122850>
- 663 46. Zhang, Z., Zhu, Z., Shen, B., Liu, L., 2019. Insights into biochar and hydrochar  
664 production and applications: A review. *Energy*.  
665 <https://doi.org/10.1016/j.energy.2019.01.035>
- 666 47. Zhen, G., Lu, X., Kato, H., Zhao, Y., Li, Y.Y., 2017. Overview of pretreatment  
667 strategies for enhancing sewage sludge disintegration and subsequent anaerobic  
668 digestion: Current advances, full-scale application and future perspectives. *Renew.*  
669 *Sustain. Energy Rev.* 69, 559–577. <https://doi.org/10.1016/j.rser.2016.11.187>
- 670 48. Zhou, H., Brown, R.C., Wen, Z., 2020. Biochar as an additive in anaerobic  
671 digestion of municipal sludge: Biochar properties and their effects on the digestion  
672 performance. *ACS Sustain. Chem. Eng.* 8, 6391–6401.  
673 <https://doi.org/10.1021/acssuschemeng.0c00571>  
674  
675

676 **Figure 1.** Configuration of the 3 L stainless-steel reactor: (1) motor and mixer; (2) gas  
677 outlet; (3) closing screws; (4) discharging port; (5) silicone stopper; (6) inflow;  
678 heater connection; (8) outflow.

679



680

681

682 **Table 1.** Chemical characteristics of the mixed sludge, mixed sludge with 10 g L<sup>-1</sup> of  
 683 SS550a BC, and of the digestate. Data expressed as mean ± standard error (number of  
 684 values).

	Mixed sludge	Mixed sludge + SS550a (10 g l <sup>-1</sup> )	Digestate
pH [-]	6.1 ± 0.1 (4)	6.0 ± 0.3 (2)	7.33 ± 0.003 (1)
TS [%-wt]	3.1 ± 0.1 (4)	3.9 ± 0.1 (2)	2.51 ± 0.04 (1)
VS [%-wt]	2.0 ± 0.1 (4)	2.2 ± 0.2 (2)	1.36 ± 0.03 (1)
VS/TS [%-wt]	64 ± 2.0 (4)	55 ± 2.4 (2)	54.3 ± 0.1 (1)
tCOD [g L <sup>-1</sup> O <sub>2</sub> ]	35 ± 2 (4)	38 ± 6 (2)	21.0 ± 0.7 (1)
sCOD [g L <sup>-1</sup> O <sub>2</sub> ]	2.0 ± 0.5 (4)	2.6 ± 0.7 (2)	0.34 ± 0.04 (1)

685

**Figure 2.** Biogas, methane and carbon dioxide productions during the semi-continuous AD of mixed sludge with and without SS550a biochar: (A) Gas production as  $\text{NmL d}^{-1}$ ; (B) Gas production as  $\text{NmL g tCOD}^{-1} \text{d}^{-1}$ ; (C) Gas production as  $\text{NmL g VS}^{-1} \text{d}^{-1}$ ; (D)  $\text{CH}_4$ ,  $\text{CO}_2$ , and  $\text{H}_2\text{S}$  concentration; (E) Organic loading rate as  $\text{gVS L}^{-1} \text{d}^{-1}$  and  $\text{g tCOD L}^{-1} \text{d}^{-1}$

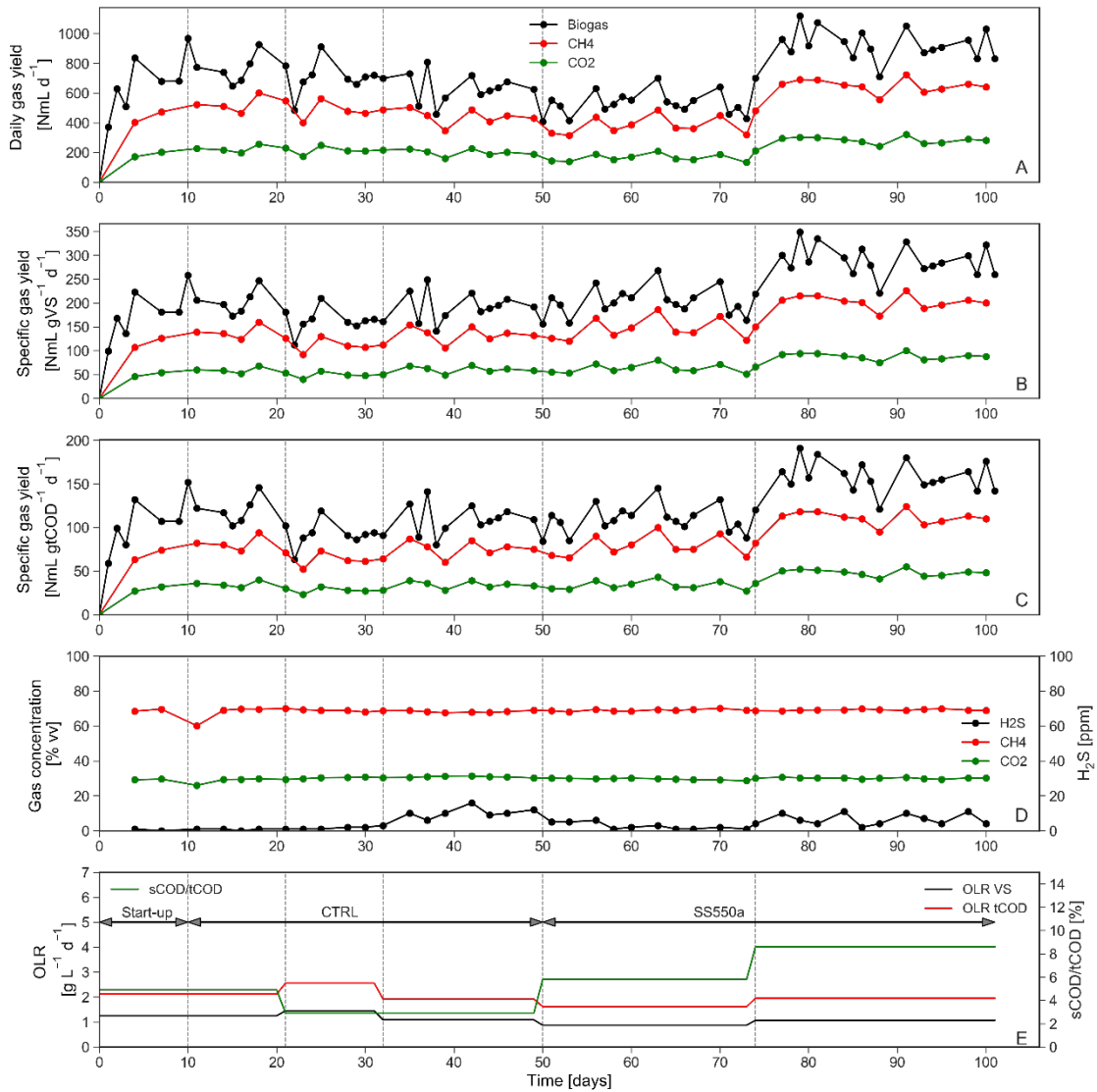


**Table 2.** Summary of the experimental results of the semi-continuous AD test, in each phase, reported as mean (standard error).

		CTRL			SS550a	
		Phase 1 (day 10-20)	Phase 2 (day 21-31)	Phase 3 (day 32-49)	Phase 4 (day 50-73)	Phase 5 (day 74-101)
Biogas properties	Biogas [NmL d <sup>-1</sup> ]	791 (45)	707 (37)	637 (28)	527 (18)	917 (26)
	Biogas [NmL g <sub>VS</sub> <sup>-1</sup> d <sup>-1</sup> ]	211 (12)	163 (9)	191 (9)	202 (7)	286 (8)
	Biogas [NmL g <sub>COD</sub> <sup>-1</sup> d <sup>-1</sup> ]	125 (7)	92 (5)	108 (5)	109 (4)	157 (4)
	Methane [NmL d <sup>-1</sup> ]	525 (28)	491 (30)	445 (18)	379 (19)	636 (19)
	Methane [NmL g <sub>VS</sub> <sup>-1</sup> d <sup>-1</sup> ]	140 (7)	113 (7)	132 (6)	145 (7)	198 (6)
	Methane [NmL g <sub>COD</sub> <sup>-1</sup> d <sup>-1</sup> ]	83 (4)	64 (4)	75 (3)	78 (4)	109 (3)
	CO <sub>2</sub> [NmL d <sup>-1</sup> ]	224 (12)	214 (12)	201 (8)	163 (8)	277 (9)
	CO <sub>2</sub> [NmL g <sub>VS</sub> <sup>-1</sup> d <sup>-1</sup> ]	60 (3)	49 (3)	60 (3)	62 (3)	86 (3)
	CO <sub>2</sub> [NmL g <sub>COD</sub> <sup>-1</sup> d <sup>-1</sup> ]	35 (2)	28 (2)	34 (2)	34 (2)	47 (1)
	CH <sub>4</sub> [% vv]	67.1 (2.3)	69.0 (0.3)	68.2 (0.2)	68.9 (0.2)	69.1 (0.1)
	CO <sub>2</sub> [% vv]	28.6 (0.9)	30.1 (0.2)	30.8 (0.1)	29.6 (0.2)	30.1 (0.1)
	H <sub>2</sub> S [ppm vv]	0.8 (0.3)	1.4 (0.2)	9.5 (1.4)	2.7 (0.6)	6.4 (0.9)
Digestate properties	TS [%]	2.9 (0.1)	3.2 (0.2)	3.3 (0.1)	3.5 (0.1)	3.6 (0.1)
	VS [%]	1.6 (0.04)	1.8 (0.1)	1.9 (0.1)	1.9 (0.02)	1.9 (0.1)
	VS/TS [%]	56.3 (0.1)	57.0 (0.8)	57.3 (0.2)	53.2 (1.0)	52.8 (0.5)
	pH [-]	7.2 (0.1)	7.1 (0.1)	6.9 (0.1)	7.1 (0.1)	7.1 (0.03)
	tCOD [g L <sup>-1</sup> ]	22 (4)	30 (3)	32 (1)	30.5 (0.4)	32 (1)
	sCOD [mg L <sup>-1</sup> ]	541 (128)	637 (51)	730 (43)	645 (43)	675 (53)
	Ammonia Nitrogen [mg L <sup>-1</sup> ]	505 (3)	442 (29)	463 (6)	505 (19)	534 (17)
	Organic Acids [mg L <sup>-1</sup> CH <sub>3</sub> COOH]	117 (13)	204 (23)	233 (16)	200 (15)	208 (21)
	Electrical conductivity [mS cm <sup>-1</sup> ]	4.5 (0.1)	4.1 (0.1)	4.4 (0.2)	4.6 (0.1)	5.1 (0.1)
	Total Alkalinity [mg L <sup>-1</sup> CaCO <sub>3</sub> ]	2900 (25)	2764 (145)	2721 (51)	2997 (108)	3293 (47)
	TS removal [%]	5 (2)	9 (2)	5 (1)	12 (4)	16 (4)
	VS removal [%]	12 (2)	21 (1)	17 (1)	11 (3)	21 (3)
	tCOD removal [%]	29 (11)	28 (1)	20 (1)	10 (6)	32 (3)
	sCOD removal [%]	65 (8)	43 (5)	35 (4)	67 (4)	80 (2)



**Table 3.** Results of multiple linear regression to predict biogas and anaerobic digestate parameters based on OLR as sCOD ( $\text{g sCOD L}^{-1} \text{d}^{-1}$ ) and biochar concentration ( $\text{g L}^{-1}$ ). The linear model is expressed in the form  $y = b_0 + b_1 x_1 + b_2 x_2$ , where  $y$  is the estimated parameter,  $x_1$  is the OLR,  $x_2$  is the BC concentration.

	Dependent variable (y)	df regression	df residuals	F	p	R <sup>2</sup>	b <sub>0</sub>	p <sub>0</sub>	b <sub>1</sub>	p <sub>1</sub>	b <sub>2</sub>	p <sub>2</sub>
Biogas properties	Biogas [ $\text{NmL d}^{-1}$ ]	2	61	68.96	2.2E-16	0.693	330.5	6.6E-13	4898.3	3.8E-17	-24.60	3.4E-09
	Biogas [ $\text{NmL gvs}^{-1} \text{d}^{-1}$ ]	2	61	50.94	9.8E-14	0.625	111.4	3.4E-13	999.6	1.1E-09	0.24	0.84
	Methane [ $\text{NmL d}^{-1}$ ]	2	36	48.52	6.0E-11	0.729	245.5	2.7E-10	3182.7	1.7E-11	-15.13	5.6E-06
	Methane [ $\text{NmL gvs}^{-1} \text{d}^{-1}$ ]	2	36	37.76	1.4E-09	0.677	83.0	3.0E-10	621.3	3.0E-06	0.81	0.41
	CO <sub>2</sub> [ $\text{NmL d}^{-1}$ ]	2	36	42.47	3.4E-10	0.702	110.3	4.2E-10	1372.6	7.8E-11	-6.86	6.5E-06
	CO <sub>2</sub> [ $\text{NmL gvs}^{-1} \text{d}^{-1}$ ]	2	36	31.49	1.2E-08	0.636	37.0	6.3E-10	269.3	7.8E-06	0.24	0.59
	CH <sub>4</sub> [% vv]	2	36	1.63	0.21	0.083	68.3	1.8E-45	-1.8	0.82	0.10	0.16
	CO <sub>2</sub> [% vv]	2	36	0.41	0.67	0.022	30.3	6.3E-41	-2.3	0.64	-0.01	0.84
H <sub>2</sub> S [ppm vv]	2	36	0.12	0.89	0.006	4.4	0.03	9.3	0.68	-0.09	0.64	
Digestate properties	TS [%]	2	20	10.53	7.5E-04	0.513	3.2	1.3E-15	-1.0	0.57	0.05	0.002
	VS [%]	2	20	1.62	0.22	0.140	1.8	2.1E-15	-0.5	0.60	0.01	0.13
	VS/TS [%]	2	20	38.54	1.4E-07	0.794	56.9	1.6E-26	0.4	0.96	-0.43	6.1E-06
	pH [-]	2	20	0.56	0.58	0.053	7.0	3.9E-26	1.0	0.35	-0.004	0.69
	tCOD [ $\text{g L}^{-1}$ ]	2	20	1.25	0.31	0.111	30.4	1.4E-10	-21.7	0.47	0.38	0.15
	sCOD [ $\text{mg L}^{-1}$ ]	2	20	0.06	0.94	0.006	678.7	7.4E-08	-333.2	0.73	2.19	0.79
	Ammonia Nitrogen [ $\text{mg L}^{-1}$ ]	2	20	6.80	0.01	0.405	438.3	7.2E-14	410.3	0.16	3.11	0.21
	Organic Acids [ $\text{mg L}^{-1}$ CH <sub>3</sub> COOH]	2	19	0.50	0.61	0.050	218.8	2.1E-06	-350.2	0.37	3.04	0.37
	Electrical conductivity [ $\text{mS cm}^{-1}$ ]	2	20	18.35	3.0E-05	0.647	3.9	2.4E-16	5.0	0.02	0.03	0.08
	Total Alkalinity [ $\text{mg L}^{-1} \text{CaCO}_3$ ]	2	19	26.41	3.3E-06	0.735	2531.9	1.2E-16	3201.1	0.01	23.23	0.03
	TS removal [%]	2	18	1.39	0.28	0.133	4.7	0.37	42.1	0.47	0.28	0.58
	VS removal [%]	2	18	2.00	0.16	0.182	8.3	0.08	98.1	0.06	-0.51	0.25
	tCOD removal [%]	2	18	5.81	0.01	0.392	1.6	0.82	278.4	0.003	-1.59	0.04
	sCOD removal [%]	2	20	23.23	6.1E-06	0.699	30.8	1.3E-04	229.2	0.01	1.32	0.06

**Figure 3.** Characteristics of the digestate during the AD test: (A) total and soluble COD; (B) Total Solids and Volatile Solids; (C)

Removals of total COD and soluble COD; (D) Removals of Total Solids and Volatile Solids; (E) pH and Electrical Conductivity; (F) Total Alkalinity, Organic Acids, Ammonia Nitrogen.

